JACS
JOURNAL OF THE AMERICAN CHEMICAL SOCIETY
Communication
pubs.acs.org/JACS

Ultrastable PbSe Nanocrystal Quantum Dots via *in Situ* Formation of Atomically Thin Halide Adlayers on PbSe(100)

Ju Young Woo,[†,‡] Jae-Hyeon Ko,[§,∥] Jung Hoon Song,[†,§] Kyungnam Kim,[†] Hyekyoung Choi,[†,#] Yong-Hyun Kim,*[,§,∥,⊥] Doh C. Lee,*[,‡,⊥] and Sohee Jeong*[,†,#]

[†]Nanomechanical Systems Research Division, Korea Institute of Machinery and Materials (KIMM), Daejeon 305-343, Korea
[‡]Department of Chemical and Biomolecular Engineering, [§]Graduate School of Nanoscience and Technology, and [⊥]KAIST Institute for the NanoCentury, Korea Advanced Institute of Science and Technology (KAIST), Daejeon 305-701, Korea
[#]Department of Nanomechatronics, Korea University of Science and Technology (UST), Daejeon 305-350, Korea
[∥]Center for Nanomaterials and Chemical Reactions, Institute for Basic Science (IBS), Daejeon 305-701, Korea

Supporting Information

ABSTRACT: The fast degradation of lead selenide (PbSe) nanocrystal quantum dots (NQDs) in ambient conditions impedes widespread deployment of the highly excitonic, thus versatile, colloidal NQDs. Here we report a simple *in situ* post-synthetic halide salt treatment that results in size-independent air stability of PbSe NQDs without significantly altering their optoelectronic characteristics. From TEM, NMR, and XPS results and DFT calculations, we propose that the unprecedented size-independent air stability of the PbSe NQDs can be attributed to the successful passivation of under-coordinated PbSe(100) facets with atomically thin PbX_2 (X = Cl, Br, I) adlayers. Conductive films made of halide-treated ultrastable PbSe NQDs exhibit markedly improved air stability and behave as an *n*-type channel in a field-effect transistor. Our simple *in situ* wet-chemical passivation scheme will enable broader utilization of PbSe NQDs in ambient conditions in many optoelectronic applications.

Colloidal nanocrystal quantum dots (NQDs) garnered immense attention in the past 30 years because their size-tunable energy gaps make them uniquely suited to applications including photovoltaics,[1] solid-state lighting,[2] and lasers.[3] Interest in lead selenide (PbSe) NQDs is particularly intense because PbSe has a small bulk bandgap (0.26 eV),[4] a large exciton Bohr radius (46 nm),[5] and a high dielectric constant ($\varepsilon_m = 23$),[6] making PbSe NQDs ideal materials for various IR-active optoelectronic applications. Advances in colloidal synthesis of highly monodispersed PbSe nanocrystals faciliated use of PbSe NQDs in prototypical proof-of-concept devices,[7] including IR light-emitting diodes[8] and field-effect transistors (FETs).[9] In particular, efficient carrier multiplication[10] and hot carrier extraction[11] reported in PbSe NQDs can translate into increased photocurrents and open-circuit voltages, respectively, in photovoltaics.

Despite their promise, progress has been hampered by the instability of PbSe NQDs in ambient conditions. While studies of NQDs have expanded from examination of wet-chemical colloidal properties to integration in functional devices, most of the reported fabrication steps for PbSe NQD-based devices require air-free environments.[9,10a,12] PbSe NQDs are highly susceptible to oxidation, in which surface Pb and Se atoms react with oxygen species. This oxidation in PbSe NQDs results in uncontrollable changes in their optical and electronic properties and abrupt failure of the solar cells or FETs.

Several approaches have been reported to improve the air stability of PbSe NQDs, including inorganic shell formation,[7b,13] ligand modification,[14] and introduction of inorganic matrices.[15] Although thick shell layers could effectively protect the PbSe NQDs from oxidation, they would also hinder efficient charge transfer through them. Recently, Bae et al. reported stabilization of PbSe NQDs through reactions with molecular chlorine, Cl_2.[16] The atomically passivated PbSe NQDs exhibited stability over months in solution, but the use of chlorine as a reagent would cause rather uncontrolled surface etching. *In situ* halide passivation of Pb chalcogenide NQDs was reported recently, adapting an alternative synthetic route using Pb halide precursors.[17]

We introduce a simple step that results in drastically improved air stability of post-synthetic PbSe NQDs while minimally altering other optoelectronic properties. We simply added halide salt, e.g., NH_4Cl, to the crude solution of PbSe NQDs at the end of the standard PbO-based synthesis. The stability of halide salt-treated NQDs was compared by monitoring spectroscopic features of samples in solution, in film, and in field-induced devices. To unravel the origin of the improved stability, we also carried out transmission electron microscopy (TEM), nuclear magnetic resonance (NMR) and X-ray photoelectron spectroscopy (XPS), and density functional theory (DFT) calculations. We conclude that a thin atomic layer of, e.g., $PbCl_2$ on PbSe(100) facets is likely responsible for the improved air stability with sufficient charge-transfer ability.

For NQD synthesis, $Pb(oleate)_2$ in diphenyl ether was reacted with TOPSe (2 M) at 120−190 °C, depending on target size, as reported previoulsy.[7] For halide treatment of NQDs, NH_4Cl—one of halide salts that can be easily ionized—was added to the reaction solution after the NQD growth stopped. The mixture was then incubated for 10 min at 60 °C (see Supporting Information (SI) for detailed procedures). The appropriate

Received: April 21, 2014
Published: June 11, 2014

dx.doi.org/10.1021/ja503957r | J. Am. Chem. Soc. 2014, 136, 8883−8886

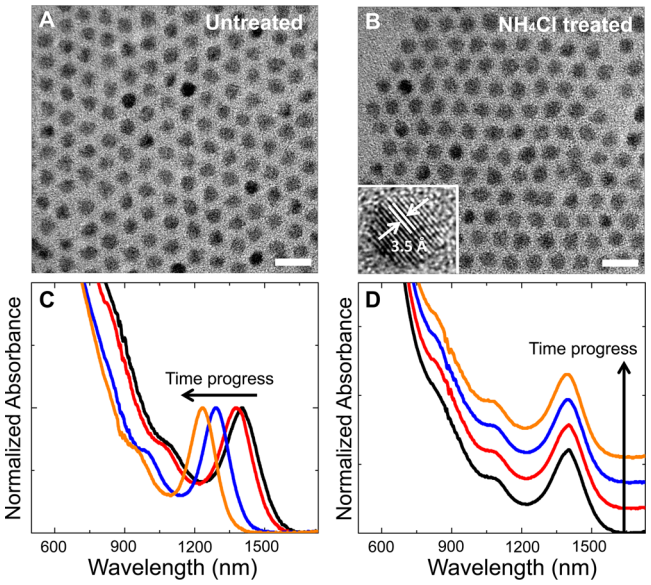

Figure 1. TEM images of (A) untreated and (B) NH_4Cl-treated PbSe NQDs (scale bars = 10 nm). The untreated and NH_4Cl-treated PbSe NQDs have sizes of 4.3 ± 0.2 and 4.4 ± 0.2 nm, respectively, and inter-NQD distances of 2.7 ± 0.1 and 2.4 ± 0.2 nm, respectively. (Inset) High-resolution TEM image of an NH_4Cl-treated PbSe NQD, showing the unchanged lattice spacing (3.5 Å) of the PbSe(111) plane. Absorption spectra of (C) untreated and (D) NH_4Cl-treated PbSe NQDs dispersed in TCE, recorded at different times after synthesis: 0 (black), 1 (red), 7 (blue), and 17 days (orange).

concentration of NH_4Cl and the incubation time were determined by varying reaction parameters for enhanced stability (Figure S1). Subsequently, unreacted precursors were removed by precipitation, and PbSe NQDs were redispersed in hexane or tetrachloroethylene (TCE) for further characterization. Figure 1A shows a TEM image of as-synthesized untreated PbSe NQDs with diameter d = 4.3 nm and size dispersion <4%. Figure 1B shows NH_4Cl-treated PbSe NQDs, which are 0.1 nm larger in size and 0.3 nm shorter in the inter-NQD distance than untreated NQDs (see Figure S2 for size analysis). The PbSe lattice spacing of NQDs was unchanged after NH_4Cl treatment (Figure 1B, inset). The oleate ligands remain almost intact after the halide treatment; the total number of bound oleate ligands is slightly reduced by 3.5%, confirmed by NMR quantification (Figure S3). The tiny reduction may be attributed to X-type ligand exchange between halide and the oleate.[18]

Figure 1C shows the absorption spectra of untreated PbSe NQDs, whose excitonic transition occurs at 1400 nm, with blue-shifts of ~170 nm after 17 days of air exposure. NH_4Cl-treated PbSe NQDs, on the other hand, resulted in an initial red-shift of <5 nm of the excitonic transition (Figure S4), and then the peak position underwent almost no change in ambient conditions for 17 days (see Figure 1D). The slight initial red-shift of the excitonic peak upon the halide treatment strongly suggests that the surface selenide is not etched, but rather is covered by a lead halide complex via Z-type addition.[19] The photoluminescence (PL) quantum yield of NH_4Cl-treated PbSe NQDs increases nearly 60% and is maintained for 21 days (Figure S5), indicating effective defect passivation by the halide treatment. The blue-shift of the absorption peak of untreated PbSe NQDs has much to do with direct surface oxidation by air. PbSe NQDs have been known to undergo structural transformations in air by forming PbO, SeO_2, and $PbSeO_3$ at the surface within a few hours.[20] The surface oxidation leads to uncontrolled size reduction (blue-shift in absorption spectra) and defect distribution, thereby significantly deteriorating the optical and electrical properties of the NQDs.[20,21]

Because the NH_4Cl treatment appears to help protect PbSe NQDs from oxidation, it is also expected to make films of the NQDs more stable. In fact, a film prepared with NH_4Cl-treated PbSe NQDs was remarkably stable, even when it was immersed in water for 18 days (Figure S6). Conductive films were then fabricated with PbSe NQDs in a layer-by-layer fashion. Insulating long-chain oleic acids were replaced with a short-chain ligand, i.e., mercaptopropionic acid (MPA), allowing the NQD films to be used for further (opto)electronic applications.[22] MPA-capped conductive films of NH_4Cl-treated PbSe NQDs exhibited a nearly unchanged excitonic peak in absorption spectra, corroborating the exceptional stability of the individual NH_4Cl-treated PbSe NQDs (Figure S7). Ethanedithiol (EDT)-passivated conductive films, on the other hand, appeared to be more susceptible to oxidation than the MPA-passivated films, possibly due to the facile desorption of EDT via hydrolysis in air, as discussed previously[23] (Figure S8).

It was recently proposed that Pb chalcogenide NQDs would show size-dependent air stability, depending on the occurrence of oleate-capped Pb-rich (111) facets and under-coordinated stoichiometric (100) facets.[24] To see the effect of the halide passivation on the size-dependent air stability, we prepared various PbSe NQDs with d = 2.1−5.5 nm, with or without NH_4Cl treatment. The excitonic peak position was monitored over time, as shown in Figure 2A. The untreated samples showed

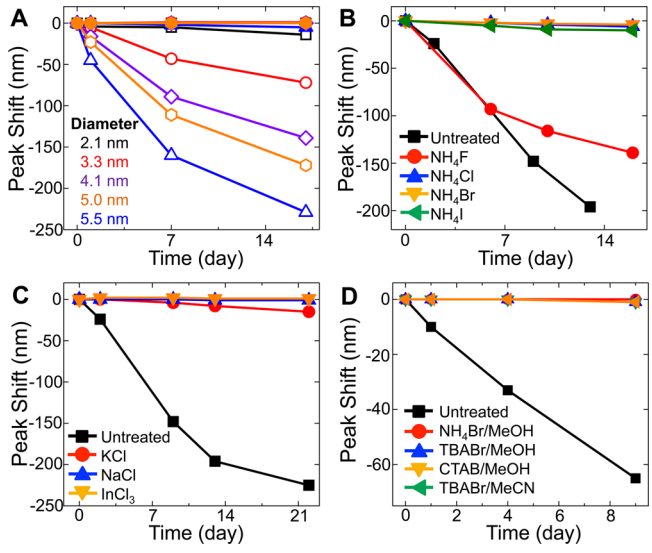

Figure 2. (A) Size-dependent absorption peak shifts of untreated PbSe NQDs (empty symbols) and NH_4Cl-treated PbSe NQDs (filled symbols) in solution over time.[25] (B) Absorption peak shifts of untreated PbSe NQDs and halide-treated PbSe NQDs with various NH_4X (X = F, Cl, Br, I) over time. (C,D) Absorption peak shifts of untreated PbSe NQDs and halide-treated PbSe NQDs with varying cations. PbSe NQDs used in (B−D) are 4.0−4.4 nm in size.

size-dependent air stability as anticipated,[24] because of the fast oxidation of the under-coordinated (100) facets for large PbSe NQDs. In contrast, all of the NH_4Cl-treated samples remained almost intact. The *size-independent* air stability strongly indicates that the halide treatment mainly affects the under-coordinated (100) facets of PbSe NQDs.

dx.doi.org/10.1021/ja503957r | J. Am. Chem. Soc. 2014, 136, 8883−8886

We extended the list of ammonium halides from chloride to bromide, iodide, and fluoride. All tested halide salts except fluoride resulted in ultrastable PbSe NQDs (Figure 2B). Halide salts with various cations were also tested. KCl, NaCl, and $InCl_3$ were almost equally effective in stabilizing PbSe NQDs (Figure 2C). NH_4Br, tetra-*n*-butylammonium bromide (TBABr), and cetyltrimethylammonium bromide (CTAB) with bulky cations made no difference in stabilizing PbSe NQDs (Figure 2D). Also, TBABr dissolved in an aprotic solvent, acetonitrile, similarly stabilized PbSe NQDs. We were able to stabilize PbSe NQDs in air simply by adding virtually any halide salt at the end of wet-chemical synthetic procedures.

To ascertain the exact nature of surface passivation and surface chemistry after our halide treatment, we conducted XPS studies. XPS spectra in Figure 3A show two features from Pb $4f_{5/2}$ and

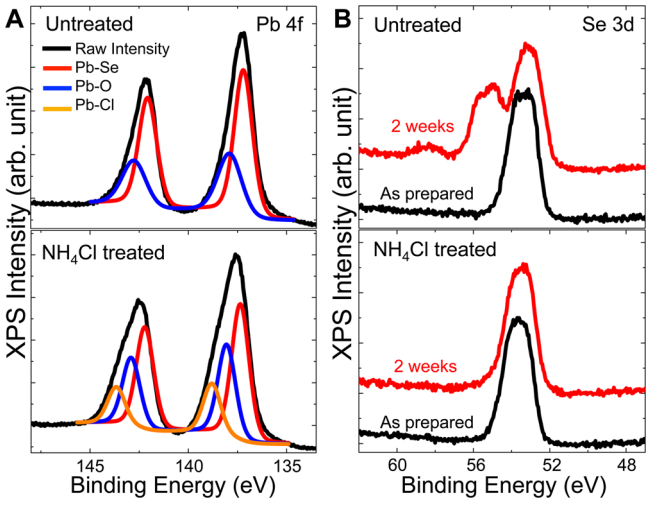

Figure 3. (A) Pb 4f core-level XPS spectra of untreated and NH_4Cl-treated PbSe NQDs (d = 4.3 nm) in air-free conditions. (B) Se 3d core-level XPS spectra of untreated and NH_4Cl-treated PbSe NQDs as prepared (black) and after 2 weeks in ambient environment (red).

$4f_{7/2}$ core levels of untreated and NH_4Cl-treated PbSe NQDs under air-free conditions. For the untreated PbSe NQDs, a relatively large population of Pb−O adducts appeared in the Pb 4f spectrum. Considering that the sample was kept air-free for the measurement, we ascribe the Pb−O peak to Pb oleate conjugation. In contrast, the Pb 4f peak in the spectrum of the NH_4Cl-treated sample is shifted to higher binding energy and broadened compared to the peak for untreated PbSe NQDs. This can be attributed to Pb−Cl bonding, as Pb−Cl has a higher binding energy (138.8 eV) than Pb−Se (137.3 eV) or Pb−O (138.0 eV).[26] The Cl 2p XPS peak was indeed detected (Figure S9). Se 3d XPS spectra in Figure 3B clearly show selenium oxidation for the untreated NQDs. The high-energy oxidation states of Se can be attributed to SeO_2 or SeO_3^{2-}.[20] NH_4Cl-treated NQDs show nearly unchanged spectra after air exposure for 2 weeks.

The under-coordinated PbSe(100) facets of NQDs are more prone to oxidation than the fully coordinated PbSe(111) facets.[24] Our experimental facts, including the size-independent air stability, strongly suggest that halide ions predominantly form an atomically thin, stoichiometric passivation layer on the PbSe(100) facets after reacting with Pb oleate precursors remaining in solution,[27] although the X-type ligand exchange on PbSe(111) could take place slightly.

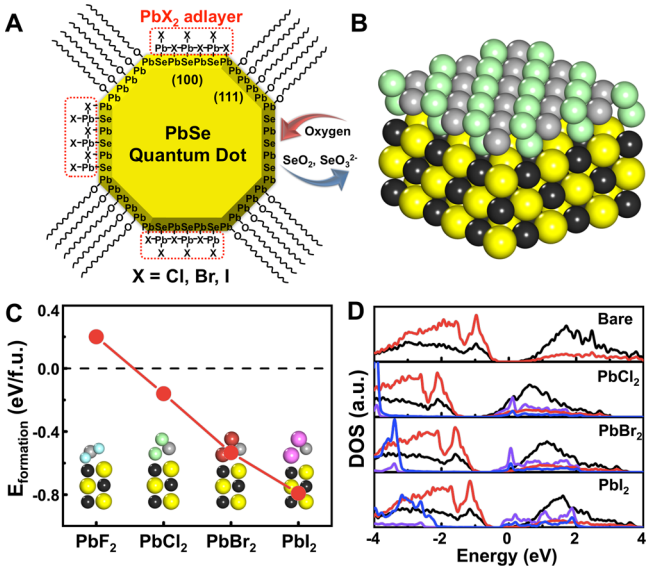

Figure 4. (A) Schematic of ultrastable, halide-treated PbSe NQDs. (B) Atomic model of $PbCl_2$-passivated PbSe(100) surface (gray, surface Pb; black, bulk Pb; yellow, Se; green, Cl). (C) DFT formation energy of various PbX_2 adlayers on the PbSe(100) surface. (Inset) Side view of PbX_2/PbSe(100). (D) Site-projected electronic density of states (DOS) for PbX_2/PbSe(100) (purple, surface Pb; black, bulk Pb; red, Se; blue, X). Zero energy represents the mid-bandgap of bare PbSe(100) after vacuum alignment.

We propose an atomic model of atomically thin, oxidation-resistant $PbCl_2$ adlayers on PbSe(100) after the NH_4Cl treatment, as schematically shown in Figure 4A. To see the formation energetics of the protective adlayer, we performed first-principles DFT calculations for an atomic monolayer of PbX_2 (X = F, Cl, Br, I) on the PbSe(100) surface (see Figure 4B and SI). The formation energy of the PbX_2 adlayer was calculated as $E_{formation} = [E(n\mathrm{PbSe}/m\mathrm{PbX_2}) - n\mu(\mathrm{PbSe}) - m\mu(\mathrm{PbX_2})]/m$ for the (1×1) surface unit cell; E is DFT total energy, n and m represent the numbers of PbSe and PbX_2 formula units in the system, respectively, and μ represents the chemical potential. μ(PbSe) was taken for the PbSe bulk phase, and $\mu(PbX_2)$ was taken from DFT total energies of $Pb(oleate)_2$, NH_4X, oleate-H, and NH_3.

The obtained formation energies, summarized in Figure 4C, indicate that the PbX_2 adlayer, except for PbF_2, is likely to form on top of the PbSe(100) surface. The positive formation energy of the PbF_2 adlayer, indicating that it is unlikely to form, can be attributed to the discrepancy between Pb−F and Pb−Se bond lengths (Table S1), consistent with the instability of NH_4F-treated PbSe NQDs, as described in Figure 2B. Our DFT electronic structure analyses show that the energy gap of the PbX_2 adlayer has a type-II alignment with the original band gap (Figure 4D) and that the dipole field of the PbX_2 adlayer downshifts the electronic band rigidly by 0.4−1.1 eV. Halide electronic states are deeply located in electronic energy, compared to the valence band state of selenium. This means that the halide states are much less prone to oxidation than the selenium state. Thus, the PbX_2 (X = Cl, Br, I) adlayer on the PbSe(100) surface could be resistant to surface oxidation.

To evaluate the effect of the halide passivation on the characteristics of (opto)electronic NQD devices, we fabricated PbSe NQD FETs on a boron-doped silicon substrate with interdigitated array electrodes (Figure 5A inset). Gate dielectric

dx.doi.org/10.1021/ja503957r | J. Am. Chem. Soc. 2014, 136, 8883−8886

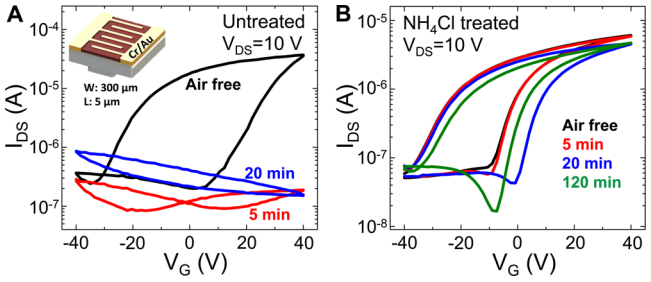

Figure 5. Transfer curves of a PbSe NQD (d = 3.7 nm) field effect transistor (A) without and (B) with NH_4Cl treatment, taken at different times after air exposure. Inset in (A) shows the device configuration.

SiO_2 was deposited on a Si wafer. The untreated and NH_4Cl-treated PbSe NQDs were deposited via spin-coating, and conductive NQD films were prepared after ligand exchange with MPA.[22] All the fabrication procedures were conducted in an inert atmosphere. As can be seen in the transfer curves (Figure 5A,B in black), the initial measurements indicate that the FET devices exhibit ambipolar and *n*-type behavior for untreated and halide-treated PbSe NQD films, repectively. The untreated NQD FETs failed shortly after air exposure. NH_4Cl-treated PbSe NQD FETs show an outstanding stability in air on a device level, nearly preserving the original *n*-type behavior. Indeed, the NQD stability transfers to the device stability. The *n*-type carriers may be generated after the NH_4Cl treatment because of the PbX_2 dipole field and thus the downshift of electronic states, as shown in Figure 4D.

In conclusion, we have developed a highly simple and versatile method that results in dramatic improvement of the air stability of PbSe NQDs. Colloidally synthesized PbSe NQDs, which are notorious for their instability in air, become stable in air for weeks after the facile halide treatment in solution. The dramatically improved stability of PbSe NQDs promises various PbSe NQD-based optoelectronic devices that can be operated in ambient conditions.

■ ASSOCIATED CONTENT

Ⓢ Supporting Information

Details about synthesis, characterization (UV−vis, PL, TEM, NMR, XPS), and DFT simulation. This material is available free of charge via the Internet at http://pubs.acs.org.

■ AUTHOR INFORMATION

Corresponding Author

yong.hyun.kim@kaist.ac.kr; dclee@kaist.edu; sjeong@kimm.re.kr

Notes

The authors declare no competing financial interest.

■ ACKNOWLEDGMENTS

This work was supported by the Global Frontier R&D program by the Center for Multiscale Energy Systems (2011-0031566) and the Global R&D program (1415134409). D.C.L. was also supported by the grant (No. 2011-0030256). J.-H.K and Y.-H.K. were also supported by IBS (CA-1201-02).

■ REFERENCES

(1) (a) Nozik, A. J. *Physica E* **2002**, *14*, 115. (b) Kamat, P. V. *J. Phys. Chem. C* **2008**, *112*, 18737. (c) Klimov, V. I. *Appl. Phys. Lett.* **2006**, *89*, 123118. (d) Sargent, E. H. *Nat. Photon.* **2012**, *6*, 133.

(2) (a) Wood, V.; Bulovic, V. *Nano Rev.* **2010**, *1*, 5202. (b) Sun, L. F.; Choi, J. J.; Stachnik, D.; Bartnik, A. C.; Hyun, B. R.; Malliaras, G. G.; Hanrath, T.; Wise, F. W. *Nat. Nanotechnol.* **2012**, *7*, 369. (c) Shirasaki, Y.; Supran, G. J.; Bawendi, M. G.; Bulovic, V. *Nat. Photon.* **2013**, *7*, 13.

(3) Schaller, R. D.; Petruska, M. A.; Klimov, V. I. *J. Phys. Chem. B* **2003**, *107*, 13765.

(4) Pietryga, J. M.; Schaller, R. D.; Werder, D.; Stewart, M. H.; Klimov, V. I.; Hollingsworth, J. A. *J. Am. Chem. Soc.* **2004**, *126*, 11752.

(5) Wise, F. W. *Acc. Chem. Res.* **2000**, *33*, 773.

(6) Romero, H. E.; Drndic, M. *Phys. Rev. Lett.* **2005**, *95*, 156801.

(7) (a) Murray, C. B.; Sun, S. H.; Gaschler, W.; Doyle, H.; Betley, T. A.; Kagan, C. R. *IBM J. Res. Dev.* **2001**, *45*, 47. (b) Pietryga, J. M.; Werder, D. J.; Williams, D. J.; Casson, J. L.; Schaller, R. D.; Klimov, V. I.; Hollingsworth, J. A. *J. Am. Chem. Soc.* **2008**, *130*, 4879.

(8) Steckel, J. S.; Coe-Sullivan, S.; Bulovic, V.; Bawendi, M. G. *Adv. Mater.* **2003**, *15*, 1862.

(9) Talapin, D. V.; Murray, C. B. *Science* **2005**, *310*, 86.

(10) (a) Semonin, O. E.; Luther, J. M.; Choi, S.; Chen, H. Y.; Gao, J. B.; Nozik, A. J.; Beard, M. C. *Science* **2011**, *334*, 1530. (b) Schaller, R. D.; Klimov, V. I. *Phys. Rev. Lett.* **2004**, *92*, 186601. (c) Nozik, A. J.; Beard, M. C.; Luther, J. M.; Law, M.; Ellingson, R. J.; Johnson, J. C. *Chem. Rev.* **2010**, *110*, 6873.

(11) Tisdale, W. A.; Williams, K. J.; Timp, B. A.; Norris, D. J.; Aydil, E. S.; Zhu, X. Y. *Science* **2010**, *328*, 1543.

(12) (a) Choi, J. J.; Lim, Y. F.; Santiago-Berrios, M. B.; Oh, M.; Hyun, B. R.; Sung, L. F.; Bartnik, A. C.; Goedhart, A.; Malliaras, G. G.; Abruna, H. D.; Wise, F. W.; Hanrath, T. *Nano Lett.* **2009**, *9*, 3749. (b) Pattantyus-Abraham, A. G.; Kramer, I. J.; Barkhouse, A. R.; Wang, X. H.; Konstantatos, G.; Debnath, R.; Levina, L.; Raabe, I.; Nazeeruddin, M. K.; Gratzel, M.; Sargent, E. H. *ACS Nano* **2010**, *4*, 3374.

(13) Lee, D. C.; Robel, I.; Pietryga, J. M.; Klimov, V. I. *J. Am. Chem. Soc.* **2010**, *132*, 9960.

(14) Hughes, B. K.; Ruddy, D. A.; Blackburn, J. L.; Smith, D. K.; Bergren, M. R.; Nozik, A. J.; Johnson, J. C.; Beard, M. C. *ACS Nano* **2012**, *6*, 5498.

(15) Liu, Y.; Gibbs, M.; Perkins, C. L.; Tolentino, J.; Zarghami, M. H.; Bustamante, J.; Law, M. *Nano Lett.* **2011**, *11*, 5349.

(16) Bae, W. K.; Joo, J.; Padilha, L. A.; Won, J.; Lee, D. C.; Lin, Q.; Koh, W. K.; Luo, H.; Klimov, V. I.; Pietryga, J. M. *J. Am. Chem. Soc.* **2012**, *134*, 20160.

(17) (a) Moreels, I.; Justo, Y.; Geyter, B. D.; Haustraete, K.; Martins, J. C.; Hens, Z. *ACS Nano* **2011**, *5*, 2004. (b) Zhang, J.; Gao, J.; Miller, E. M.; Luther, J. M.; Beard, M. C. *ACS Nano* **2014**, *8*, 614.

(18) Owen, J. S.; Park, J.; Trudeau, P. -E; Alivisatos, A. P. *J. Am. Chem. Soc.* **2008**, *130*, 12279.

(19) Anderson, N. C.; Hendricks, M. P.; Choi, J. J.; Owen, J. S. *J. Am. Chem. Soc.* **2013**, *135*, 18536.

(20) Sykora, M.; Koposov, A. Y.; McGuire, J. A.; Schulze, R. K.; Tretiak, O.; Pietryga, J. M.; Klimov, V. I. *ACS Nano* **2010**, *4*, 2021.

(21) Leschkies, K. S.; Kang, M. S.; Aydil, E. S.; Norris, D. J. *J. Phys. Chem. C* **2010**, *114*, 9988.

(22) (a) Tang, J.; Kemp, K. W.; Hoogland, S.; Jeong, K. S.; Liu, H.; Levina, L.; Furukawa, M.; Wang, X. H.; Debnath, R.; Cha, D. K.; Chou, K. W.; Fischer, A.; Amassian, A.; Asbury, J. B.; Sargent, E. H. *Nat. Mater.* **2011**, *10*, 765. (b) Ip, A. H.; Thon, S. M.; Hoogland, S.; Voznyy, O.; Zhitomirsky, D.; Debnath, R.; Levina, L.; Rollny, L. R.; Carey, G. H.; Fischer, A.; Kemp, K. W.; Kramer, I. J.; Ning, Z. J.; Labelle, A. J.; Chou, K. W.; Amassian, A.; Sargent, E. H. *Nat. Nanotechnol.* **2012**, *7*, 577.

(23) Luther, J. M.; Law, M.; Song, Q.; Perkins, C. L.; Beard, M. C.; Nozik, A. J. *ACS Nano* **2008**, *2*, 271.

(24) Choi, H.; Ko, J.-H.; Kim, Y.-H.; Jeong, S. *J. Am. Chem. Soc.* **2013**, *135*, 5278.

(25) Moreels, I.; Lambert, K.; De Muynck, D.; Vanhaecke, F.; Poelman, D.; Martins, J. C.; Allan, G.; Hens, Z. *Chem. Mater.* **2007**, *19*, 6101.

(26) Pederson, L. R. *J. Electron Spectrosc. Relat. Phenom.* **1982**, *28*, 203.

(27) Lee, S.; Lee, D. T.; Ko, J.-H.; Kim, W.-J.; Joo, J.; Jeong, S.; McGuire, J. A.; Kim, Y.-H.; Lee, D. C. *RSC Adv.* **2014**, *4*, 9842.